Int. J. Nonlinear Anal. Appl. 13 (2022) 1, 2783-2799
ISSN: 2008-6822 (electronic)
http://dx.doi.org/10.22075/ijnaa.2021.6001

Introducing a new control system based on Fuzzy-PID for controlling DFIG rotor side converter in fault conditions

Alireza Moradi[a,*], Seyed Mohammad Reza Hashemi[b]

[a]*Department of Electrical Engineering, Mahdishahr Branch, Islamic Azad University, Mahdishahr, Iran*
[b]*Faculty of Computer Engineering, Shahrood University of Technology, Shahrood, Iran*

(Communicated by Ehsan Kozegar)

Abstract

Doubly-fed induction generators are sensitive to network faults and will be isolated from the circuit when a fault occurs. According to the new rules of the network, wind turbines should be able to continue working in fault conditions and should not be isolated from the system when the network fault occurs. This article proposes a Fuzzy-PID controller for controlling the doubly-fed induction generator rotor side converter in fault conditions. This controller is only added to the circuit in fault conditions and it reduces the current of the rotor circuit with the proper control of the rotor side converter. When the network voltage is in the normal state, rotor side converter control is performed with the PI controller. The proposed method is implemented in MATLAB Simulink software. The simulation results confirm the better performance of the proposed method in the proper control of the rotor side converter in fault conditions.

Keywords: Doubly-fed induction generator (DFIG), Fault condition, Fuzzy-PID controller, Rotor side converter (RSC)

1. Introduction

Demand for electricity has been increasing dramatically in the last few years. Using new energy sources to provide electricity to consumers is a useful approach which decreases the emission of carbon and as a result, reduces global warming. Among the new energy sources, wind energy has

*Corresponding author
Email addresses: alireza.moradi@msh-iau.ac.ir (Alireza Moradi), smr.hashemi@shahroodut.ac.ir (Seyed Mohammad Reza Hashemi)

Received: June 2021 *Accepted:* September 2021

attracted more attention due to its relatively lower costs, less maintenance and less pollution [9]. Doubly fed induction generators (DFIGs) have been used extensively for their advantages among the various types of wind turbine generators. Unfortunately, DFIGs are very sensitive to network voltage disturbances, especially network faults. When a fault occurs, the amplitude and frequency of the induction voltage in the rotor circuit vary greatly and become several times higher than normal state [1]. Under these circumstances, the conventional DFIG control systems (which are based on the PI controller [12]) cannot send proper control signals to rotor side converter (RSC). Therefore, when a fault occurs, DFIG protection system blocks RSC in order to curtail damage to the electronic converters and subsequently, removes the wind turbine from the circuit [13]. But the removal of DFIG from the circuit contradicts the recent rules of the network. According to the latest regulations for network, at the time of fault occurrence, large wind farms should be connected to the network [7, 16].

In [2], authors try to enhance the stability, robustness and dynamic response of DFIG system tested in different disturbances if stator voltage changes with a genetic algorithm (GA)-based linear quadratic regulator (LQR) controller. The comprehensive model has been depicted by a state-space model. This contributes to the optimal control of all of the states by using the full-state feedback LQR controller. In order for the optimal tuning of the Q and R matrices, GA is utilized in the LQR algorithm. The results of the proportional integral (PI) and LQR controllers are used in the analogy with the dynamic response of the presented controller to evaluate the effectiveness.

The scholars have included capacitive energy storage (CES)/DFIG units and thyristor controlled phase shifter (TCPS) in both controllers to optimize the dynamic responses of frequency alternations of the area after a slight load disconcertion. Inertial support was used by modified control scheme for exploring the DFIGs behavior to improving the power system dynamic performances which was presented. As the load in the power system is changed abruptly, the control scheme response to frequency vibrations is proportional and it uses the kinetic wind turbine energy as inertial control support in different conditions of operation. The integral square error technique is employed in order to achieve the integral controller gain parameters [4].

The sensitivity of wind turbines (WTs) with DFIGs is very high when faced with abrupt changes of stator voltage because they are in direct connection with the grid. The stator current increases in fault conditions. Additionally, Due to the magnetic coupling between the stator and the rotor windings causes the induction of high rotor inrush currents that are potentially high risk for the RSC and can bring about the overvoltage of DC-link capacitor. The latest standards of grid demand that WTs and grid be linked to each other and ensure system stability at the time of grid faults and after those. To enhance the fault ride by DFIG-based WTs, they use the sliding mode control strategy as well as the control of converters on grid sides and rotor. Additionally, for the DC-link voltage control in fault conditions, a sliding mode control model which is designed on the basis of the input-output feedback linearization is proposed [15].

Another research [3], for enhancing the small signal stability uses model predictive control (MPC) in a large-scale network. Laguerre function is the basis of predictive strategy for the purpose of reducing the time of computation in MPC and augmenting the control signals detection in an exact way. The active and reactive power control on RSC is important in implementing the strategy and also is increasing RSC yield by the application of proper switching to inverter when there exist uncertainties. Thus, in the UK large-scale systems, the inter area oscillations will be reduced as the static synchronous compensators are employed in a way to compensate for the reactive power by designing a damping controller [3].

The vast application of crowbars by far has been used in limit the fault current. A series of resistors connected in parallel with rotor windings is named crowbar and they bypasses the rotor winding circuit in fault conditions and prohibits RSC from fault current. On the other hand, as the

crowbar is added to the circuit, DFIG becomes a regular induction generator and absorbs reactive power from the network. In addition, the ability to control wind turbine power production is also limited [9]. In [10, 5], a method is proposed to improve the speed of crowbar performance; however, there is still the problem of reactive power absorption. In [6], the network-side converter control method is suggested to improve DFIG performance in fault conditions. This method suffers from the complexity of the control plan and the lack of coordination in controlling the fault and normal operation of DFIG. Another research [8], proposes a dynamic resistor which connected in series with the rotor. This method reduces system reliability and causes problems in thermal aspects. In addition, the fault current that passes through these resistors creates high voltages that disrupt RSC operation. In [14], applications of integral sliding mode control (ISMC) will be checked for the fault ride-through (FRT) enhancement of the DFIG wind power system.

In this article, a Fuzzy control system is proposed to make the DFIG capable of passing a fault. Before an error occurs on the network, a conventional PI controller based on [12] controls the RSC. When the fault occurs, the normal control system is removed from the circuit and is replaced with the proposed fault control system. After the fault is resolved, the normal control system re-enters the circuit and replaces the fault control system. The proposed fault control system controls the amplitude of the rotor current when it enters the circuit and prevents it from getting too high. In the proposed method of this paper, it is not necessary to install any hardware tools such as crowbar or dynamic resistor.

Structure of the article is as follows: 2th chapter presents the state-space of the DFIG. The proposed Fuzzy-PID controller is described in 3th chapter. 4th, 5th chapters are simulation results and conclusion, respectively.

2. State-space of the DFIG

By regarding the d and q components of the stator and rotor currents as state variables of the system and the d and q components of the stator and rotor voltages as the system inputs, the state-space of DFIG in the reference frame of the synchronous (dq) will be as follows [1]:

$$\dot{x} = Ax + Bu$$

$$x = \begin{bmatrix} i_{ds} \\ i_{qs} \\ i_{dr} \\ i_{qr} \end{bmatrix}, \qquad u = \begin{bmatrix} v_{ds} \\ v_{qs} \\ v_{dr} \\ v_{qr} \end{bmatrix} \tag{1}$$

$$A = \left(\frac{1}{\sigma L_s L_r}\right) \times \begin{bmatrix} -R_s L_r & \omega_m L_m^2 + \omega_s \sigma L_s L_r & R_r L_m & \omega_m L_m L_r \\ -\omega_m L_m^2 - \omega_s \sigma L_s L_r & -R_s L_r & -\omega_m L_m L_r & R_r L_m \\ R_s L_m & -\omega_m L_s L_m & -R_r L_s & -\omega_m L_r L_s - \omega_s \sigma L_s L_r \\ \omega_m L_r L_s & R_s L_m & \omega_m L_r L_s - \omega_s \sigma L_s L_r & -R_r L_s \end{bmatrix}$$

$$B = \begin{bmatrix} \frac{L_r}{\sigma L_s L_r} & 0 & -\frac{L_m}{\sigma L_s L_r} & 0 \\ 0 & \frac{L_r}{\sigma L_s L_r} & 0 & -\frac{L_m}{\sigma L_s L_r} \\ \frac{L_m}{\sigma L_s L_r} & 0 & -\frac{L_s}{\sigma L_s L_r} & 0 \\ 0 & -\frac{L_m}{\sigma L_s L_r} & 0 & -\frac{L_s}{\sigma L_s L_r} \end{bmatrix}$$

where x is the state variables vector, u is the inputs vector, A is the state matrix and B is the input matrix. i_{ds} and i_{qs} are the currents of d and q axes of the stator, i_{dr} and i_{qr} are the currents of d

and q axes of the rotor, v_{ds} and v_{qs} are the voltages of d and q axes of the stator, v_{dr} and v_{qr} are the voltages of d and q axes of the rotor. L_s is the stator inductance and L_r is the rotor inductance, L_m is the magnetizing inductance, σ is the leakage factor, $\omega_{\mathbf{s}}$ is the angular frequency of the network voltage and $\omega_{\mathbf{m}}$ is the angular frequency of the electrical rotation of the rotor.

From a control perspective, since the stator is directly connected to the network, its terminal voltages are dependent on the network voltage and cannot be controlled by the DFIG electronic converters. On the other hand, the rotor windings via brush and slip rings are connected to the rotor side converter. Therefore, by controlling the output voltage of the rotor side converter, its voltage can be controlled.

3. Fuzzy-PID controller

The Fuzzy-PID controller is obtained by combining the adaptive nature of the Fuzzy controller and the fast response characteristics of the proportional integral controller. In these controllers, the Fuzzy logic simultaneously determines the proportional (K_P), integral (K_D), and derivative (K_D) gains of the proportional-integral controller based on the system operation point. Therefore, the dependence of the controller on the parameters changes the system; hence, external influences can be minimized, the dynamic response becomes faster and the stability increases.

The PID controller transfer function is:

$$C(S) = K_P + \frac{K_I}{S} + K_D S \tag{2}$$

Or

$$C(S) = \frac{K_D S^2 + K_P S + K_I}{S} \tag{3}$$

where K_P, K_I and K_D are proportional, integral and derivative coefficients, respectively. In the Fuzzy-PID controller, the K_P, K_I and K_D the PID controller coefficients are dynamically adjusted by a Fuzzy system. This controller's general structure is shown in Fig. 1.

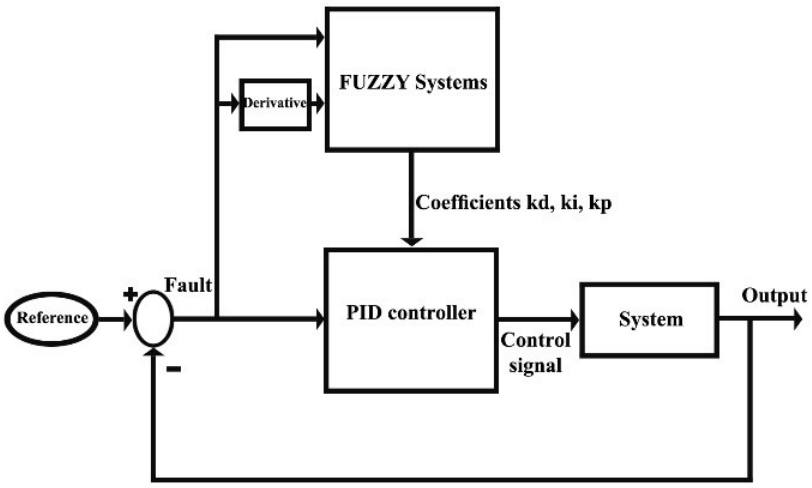

Figure 1: Fuzzy-PID controller

The Fuzzy system has two inputs and three outputs: the inputs are error and derivation of error and the outputs are K_P, K_I and K_D coefficients.

3.1. Formulate

The PID controller transfer function is as follows:

$$G_C(S) = K_P + \frac{K_I}{S} + K_D S \tag{4}$$

where K_P, K_I and K_D are the coefficients of proportional, integral, and derivative controllers, respectively. Equation (4) can also be written as follows:

$$G_C(S) = K_P(1 + \frac{1}{(T_i s)} + T_d S) \tag{5}$$

$$T_i = K_p/K_i \tag{6}$$

$$T_d = K_d/K_p \tag{7}$$

where T_i and T_d are known as the time constants of integral and derivative. The discrete equations of the PID controller are as follows:

$$u(k) = K_P e(k) + K_i T_s \sum_{i=1}^{n} e(i) + \frac{K_d}{T_s}\Delta e(k) \tag{8}$$

$$\Delta e(k) = e(k) - e(k-1) \tag{9}$$

where u(k) is the control signal, e(k) is the error between process output and reference, and T_s is the sampling period of the controller. PID controller parameters can be manually determined (Coefficients K_p , K_i and K_d or K_p, T_i andT_d) in order to obtain different response curves for a process. It is not easy to find the optimal settings of PID controller parameters for a specific process. In the next section, the adaptive design of the PID controller based on fuzzy rules will be described.

3.2. Fuzzy adjustment of PID controller coefficients

Fig. 1 exhibits the PID control system along with Fuzzy adjustment coefficients. In the following, the adopted method to Fuzzy control of PID controller coefficients is described.

We assume K_p and K_d are in the ranges of $[K_{p,min}, K_{p,max}]$ and $[K_{d,min}, K_{d,max}]$ respectively. The appropriate range is determined empirically. For simplicity, K_p and K_d are normalized to a linear relationship ranging from 0 to 1:

$$K_p^{'} = (K_p - K_{p,min})/(K_{p,max} - K_{p,min}) \tag{10}$$

$$K_d^{'} = (K_d - K_{d,min})/(K_{d,max} - K_{d,min}) \tag{11}$$

where $K_p^{'}$ and $K_d^{'}$ are the normalized values of K_p and K_d, respectively.

The Fuzzy system which calculates the triple coefficients has two inputs, which are error ($e(k)$) and its first derivative ($\Delta e(k)$). It is assumed that the relationship between the integral time constant and the derivative time constant is as follows:

$$T_i = \alpha T_d \tag{12}$$

With this assumption, integral gain is calculated with the following equation:

$$K_i = \frac{K_p}{\alpha T_d} = \frac{K_p^2}{\alpha K_d} \tag{13}$$

The $K_p^{'}$ and $K_d^{'}$ parameters and α are obtained by a series of Fuzzy rules of frequency as follows:

if $e(k)$ is A_i and $\Delta e(k)$ isB_i then $K_p^{'}$ is C_i, $K_d^{'}$ is D_i and $\alpha = \alpha_i, i = 1, 2, \ldots, m$ (14)

In the Eq. (14), A_i, B_i, C_i andD_i are Fuzzy sets corresponding to variables, and α_i is a constant number. (The Fuzzy set of the output variable α is composed of integers). m is the total number of Fuzzy rules (equal to 49).

The membership functions (MF) corresponding to $e(k)$ and $\Delta e(k)$ (Fuzzy sets A_i and B_i) are shown in Fig. 2.

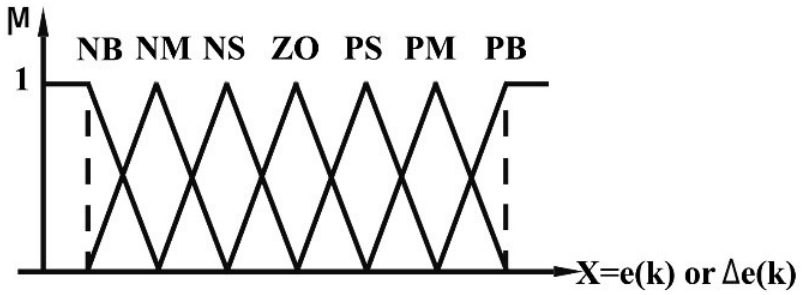

Figure 2: Membership functions for input variables $e(k)$ and $\Delta e(k)$

In Fig. 2, the vertical axis (μ) shows the degree of membership and its range is between 0 and 1. As shown in Fig. 2, $e(k)$ and $\Delta e(k)$ have 7 membership functions. In Fig. 2, N stands for Negative, P for Positive, ZO for Zero, S for Small, M for Medium, and B stands for Big.

The C_i andD_i Fuzzy sets have two Big and/or Small membership functions which are used in Fig. 3 to express the output variables $K_p^{'}$ and $K_d^{'}$.

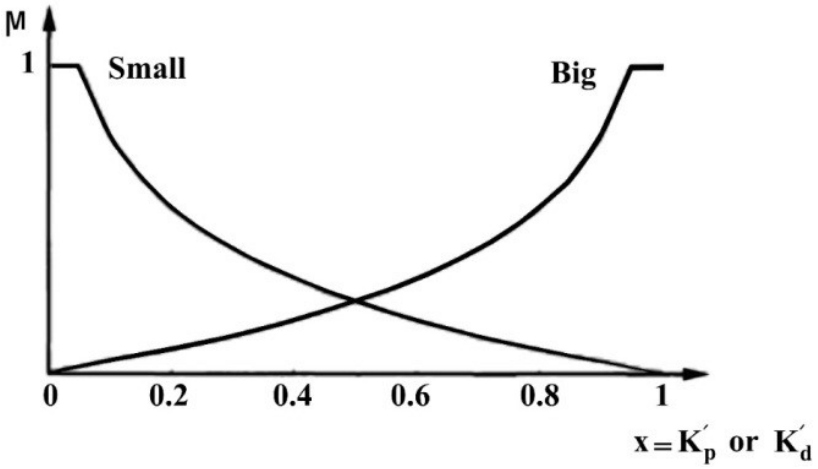

Figure 3: The membership functions corresponding to the output variables $K_p^{'}$ and $K_d^{'}$

The relationship between the degree of membership (μ) and the variable x ($K_p^{'} or K_d^{'}$) for two Small and Big membership functions is given below:

$$\mu_{Small}(x) = -\frac{1}{4} ln(x) \ or \ x_{Small}(\mu) = e^{-4\mu} \tag{15}$$

$$\mu_{Big}(x) = -\frac{1}{4} ln(1-x) \ or \ x_{Big}(\mu) = 1 - e^{-4\mu} \tag{15}$$

where μ_{Small} is the degree of membership corresponding to the Small membership function and μ_{Big} is the degree of membership corresponding to the Big membership function. The Fuzzy rules mentioned in the Eq. (14) are determined based on the experience of working with the PID controller. Here, based on the stage response of the system, Fuzzy rules are extracted. Fig. 4 shows the time response of a system.

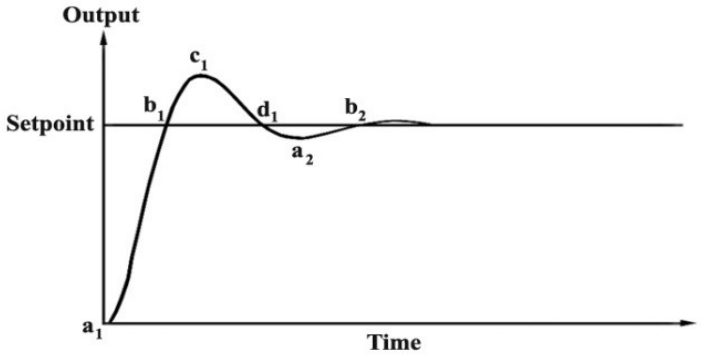

Figure 4: The step response of a system

At starting point, i.e. point a_1, a large control signal is essential for reducing the rise time. To generate a large control signal, the PID controller should have a large proportional gain, a large integrative gain, and a small derivative gain. Therefore, in this case, we can show the proportional gain ($K_p^{'}$) by the Big Fuzzy set while the derivative gain ($K_d^{'}$) can be represented by the small Fuzzy set. Using the Eq. (12), the integrative gain can be calculated using the derivative gain. For a PID controller, the consideration of a small α or a low integral time constant (T_i) leads to strong integration. The decision about the strength of the integration is made via the famous Ziggler-Nichols principle. In Ziggler-Nichols principle, the integral time constant (T_i) is at all times 4 times higher than the derivative constant which means$\alpha = 4$.

In [11], the parameter α is considered less than 4 (e.g. 2) to create a stronger integration process. Therefore, the rule a_1 is expressed as follows:

if $e(k)$ is PB and $\Delta e(k)$ is ZO then $K_p^{'}$ is Big, $K_d^{'}$ is Small and $\alpha = 2$ (17)

Note that the variable α can be expressed as a Fuzzy number with singleton membership functions. Fig. 5 shows membership functions corresponding to it. For example, when α is Small, it means it is equal to 6 and vice versa.

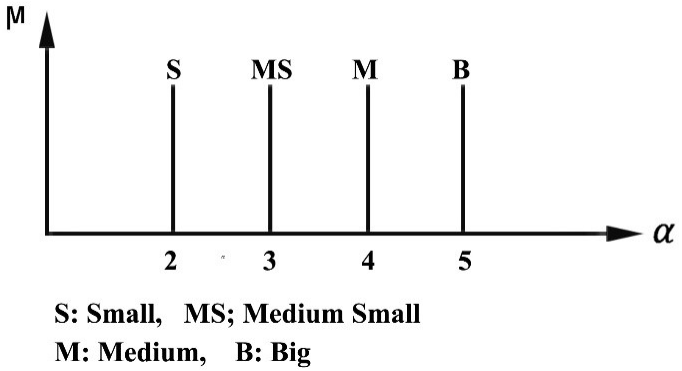

Figure 5: Singleton membership functions for the variable α

Around the point b_1 in Fig. 4, the control signal must be small to avoid high overshoot. To achieve this purpose, there should be a Small proportional gain, a large derivative gain, and a Small integral gain in PID controller; so, the below fuzzy rule is considered:

if $e(k)$ is ZO and $\Delta e(k)$ is NB, then $K_p^{'}$ is Small, $K_d^{'}$ is Big and $\alpha = 5$ (18)

Therefore, a number of rules, such as Table 1, are required to determine $K_p^{'}$ in different operating conditions. The Fuzzy rules for determining the values of $K_d^{'}$ are in Table 2 and α is also given in Table 3.

Table 1: The fuzzy rules associated with $K_p^{'}$

		Δe(k)						
		NB	NM	NS	ZO	PS	PM	PB
e(k)	NB	B	B	B	B	B	B	B
	NM	S	B	B	B	B	B	S
	NS	S	S	B	B	B	S	S
	ZO	S	S	S	B	S	S	S
	PS	S	S	B	B	B	S	S
	PM	S	B	B	B	B	B	S
	PB	B	B	B	B	B	B	B

Table 2: The fuzzy rules associated with $K_d^{'}$

		Δe(k)						
		NB	NM	NS	ZO	PS	PM	PB
e(k)	NB	S	S	S	S	S	S	S
	NM	B	B	S	S	S	B	B
	NS	B	B	B	S	B	B	B
	ZO	B	B	B	B	B	B	B
	PS	B	B	B	S	B	B	B
	PM	B	B	S	S	S	B	B
	PB	S	S	S	S	S	S	S

Table 3:): The fuzzy rules associated with α

		Δe(k)						
		NB	NM	NS	ZO	PS	PM	PB
e(k)	NB	2	2	2	2	2	2	2
	NM	3	3	2	2	2	3	3
	NS	4	3	3	2	3	3	4
	ZO	5	4	3	3	3	4	5
	PS	4	3	3	2	3	3	4
	PM	3	3	2	2	2	3	3
	PB	2	2	2	2	2	2	2

The value of the rule (i) (μ_i) in Eq. (14) to the multiplication of the membership functions values is obtained from the predefined condition:

$$\mu_i = \mu_{A_i}[e(k)].\mu_{Bi}[\Delta e(k)], i = 1, 2, \ldots, m = 49 \tag{19}$$

where μ_{A_i} is the value of the Fuzzy set membership function A_i (corresponding to the error value$e(k)$) and μ_{B_i} is the value of the Fuzzy set membership function B_i (corresponding to the derivative of the error $\Delta e(k)$.

Values of $K_p^{'}$ and $K_d^{'}$ for each of the rules are determined for their associated membership functions based on μ_i. The process of a Fuzzy rule is shown in Fig. 6.

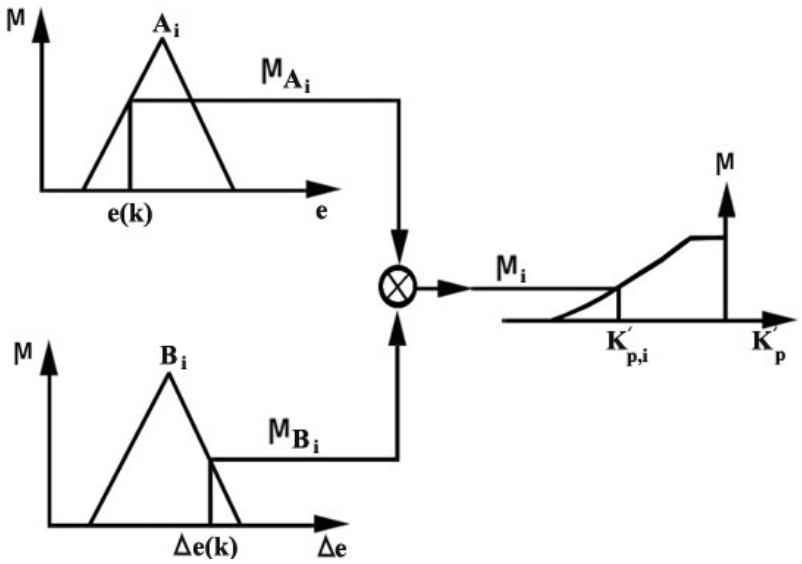

Figure 6: The Fuzzy rule process

Then, defuzzification is achieved by:

$$K_p^{'} = \sum_{i=1}^{m} z_i \mu_i K_{p,i}^{'} \tag{20}$$

$$K_d^{'} = \sum_{i=1}^{m} z_i \mu_i K_{d,i}^{'} \tag{21}$$

$$\alpha = \sum_{i=1}^{m} z_i \mu_i \alpha \tag{22}$$

As noted above, $K_{p,i}^{'}$ is the value of $K_p^{'}$ matching the value μ_i in the i_{th} rule as shown in Fig. 6 and $K_{d,i}^{'}$ is the value of $K_d^{'}$ matching the value μ_i in the i_{th} rule. When $K_p^{'}, K_d^{'}$ and α are obtained, the PID controller parameters are calculated with the following relationships which have been derived from the Eqs. (10) to (13):

$$K_p = (K_{p,max} - K_{p,min})K_p^{'} + K_{p,min} \tag{23}$$

$$K_d = (K_{d,max} - K_{d,min})K_d^{'} + K_{d,min} \tag{24}$$

$$K_d = (K_{d,max} - K_{d,min})K_d^{'} + K_{d,min} \tag{25}$$

Based on the studies extensive simulation type in diverse processes, an empirical rule for determining the range of K_p and K_d is as follows:

$$K_{p,min} = 0.32K_u \tag{26}$$
$$K_{p,max} = 0.6K_u \tag{27}$$
$$K_{d,min} = 0.08K_uT_u \tag{28}$$
$$K_{d,max} = 0.15K_uT_u \tag{29}$$

where K_u and T_u are empirically obtained. As one of the methods for calculating these two parameters, the controller must be only in the proportional state in order to obtain K_u and T_u, i.e., K_d and K_i are zero. In this case, the value of K_p is increased to generate an undamped oscillation in the system output (complete sinusoidal) and the system is on the verge of stability and instability. In this case, K_P is equal to K_u and T_u is the system oscillation period.

4. Simulation

In order to evaluate the performance of the control system employed in this research, this control system in a 1.5 MW DFIG connected to the network is simulated in MATLAB Simulink software.

In the following, two scenarios about the system under study will be examined.

Scenario 1: In case of occurrence single-phase to ground fault, its performance is compared with the reference PI controller [12].

Scenario 2: In case of occurrence three-phase to ground fault, its performance is compared with the reference PI controller [12].

The system which studied is a DFIG linked to the power system. The DFIG data, wind turbines and connected network are designed in accordance with [12, 11]. Table 4 shows its electrical data.

Table 4: Information of the DFIG and network

Parameters	Quantity
Rated stator voltage	575 V
Rated frequency	60 Hz
Rated Power	1.5 MVA
Stator Resistance: R_S	0.023 pu
L_{ls}	0.18 pu
Rotor Resistance: $R_r^{'}$	0.016 pu
$L_r^{'}$	0.16 pu
L_m	2.9 pu
Inertia: H	0.685 s
Pole pairs: p	3
C	10 mF

The graphical representation of the system is demonstrated in Fig. 7. DFIG connects to a 25 KV network via a 25 KV/575 V transformer and two 30-Km lines. These two lines are aligned in parallel in case a fault occurs in one of them; the other line maintains the DFIG connection to the network.

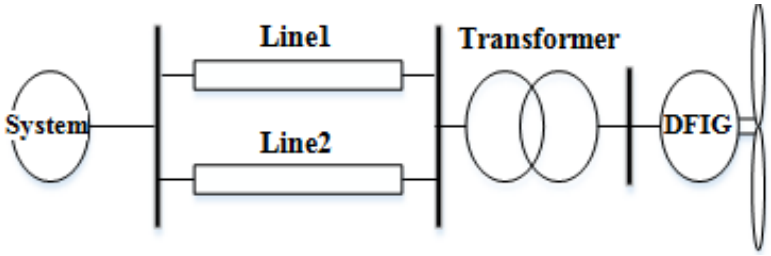

Figure 7: DFIG connected to the studied network

In the following, different scenarios about the system under study will be examined:

4.1. Scenario 1

In this scenario, the DFIG is in its normal operating state, then a single-phase to ground fault occurs at 0.9 seconds in the middle of line A (15 Km from the beginning of the line 2) as shown in Fig. 8. This fault is resolved 0.1 seconds later with the function of the relay protection. The network voltage variations are very intense in this case as shown in Fig. 9.

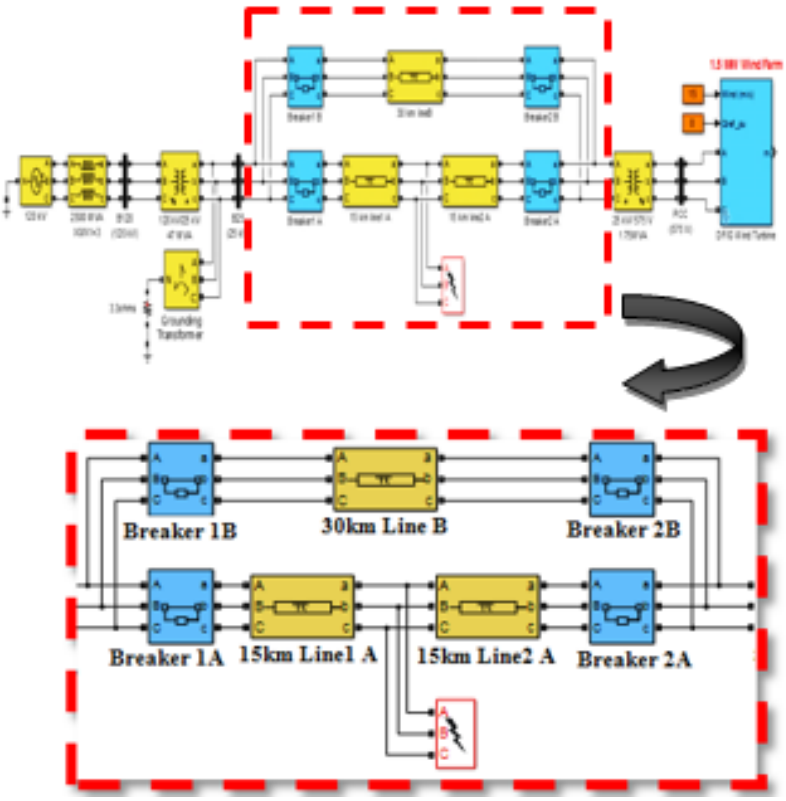

Figure 8: Short circuit fault location

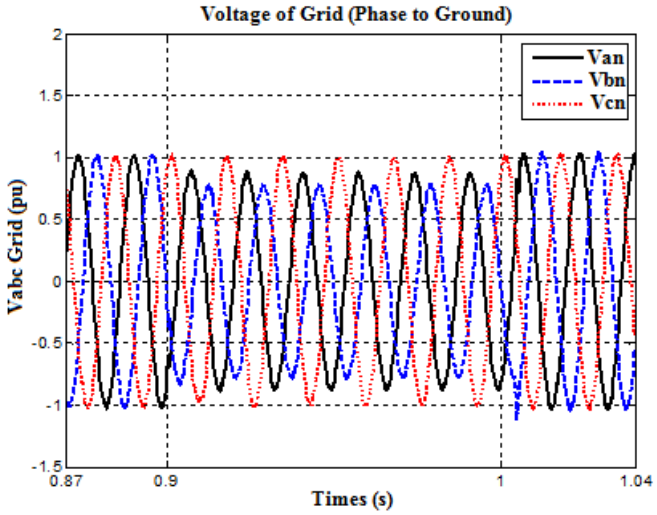

Figure 9: Network voltage in the case of a single-phase to ground fault

When an error occurs, the error observer output changes as Fig. 10.

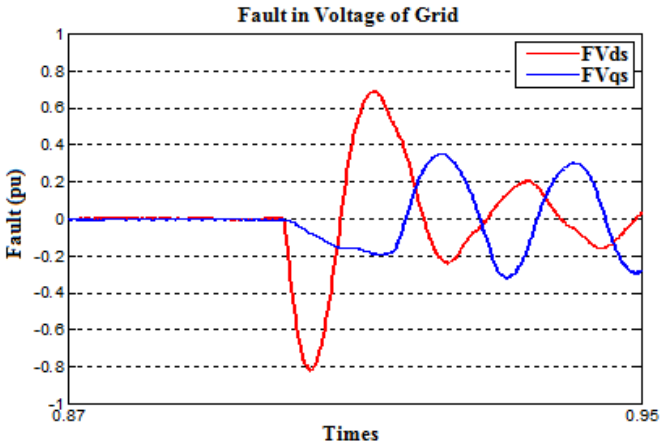

Figure 10: Error observer output changes

In the figure above, $F_{v_{ds}}$ and $F_{v_{qs}}$ are the amounts of voltage unbalanced in the d and q components of the stator voltage, respectively. These two components start to increase in 0.9 seconds due to an error in the network, and in 0.9001 seconds their range is more than 10%, so, the fault detection system issues an order to replace the controllers. At 1.0084 seconds, the network voltage returns to normal and the PI controller regains control of the DFIG rotor side converter and replaces the fault mode controller.

To compare the performance of the proposed controller based on the Fuzzy-PID controller with the PI controller in reducing the amplitude of the rotor circuit current, the current of each phase of the rotor circuit with each controller is plotted in Figs. 11 to 13. The current of the rotor in the case of being controlled with Fuzzy-PID controller and PI controller is plotted with a black line and a blue dashed line, respectively.

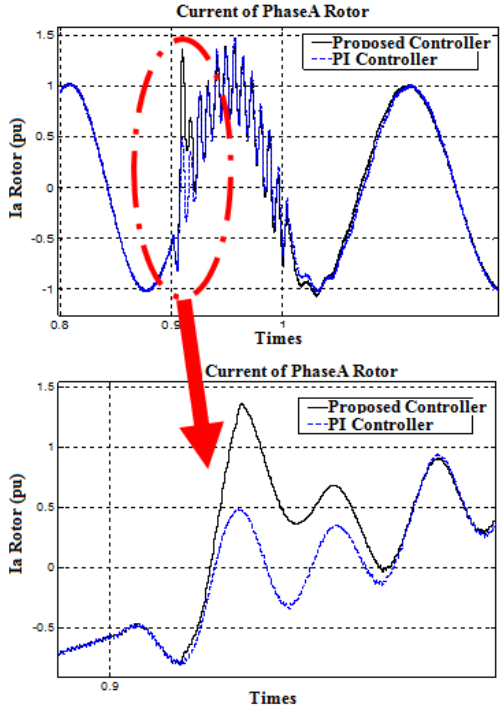

Figure 11: Comparison of the current of phase A of the rotor in the case of a single-phase to ground fault in two modes: with PI controller and proposed controller

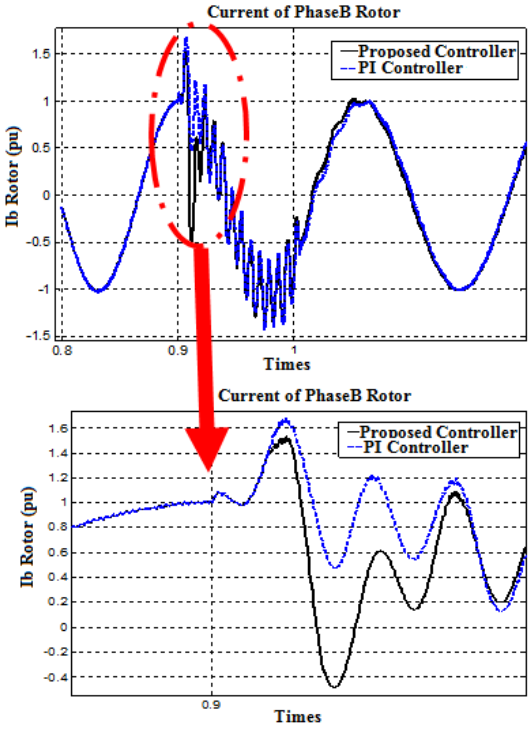

Figure 12: Comparison of the current of phase B of the rotor in the case of a single-phase to ground fault in two modes: with PI controller and proposed controller

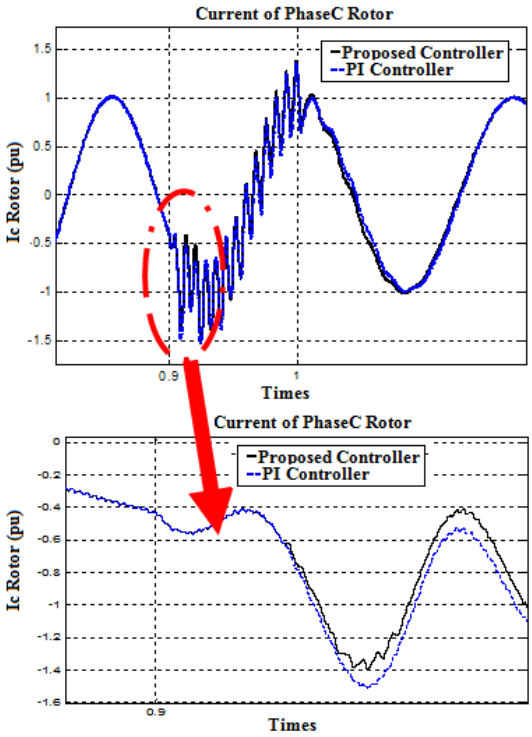

Figure 13: Comparison of the current of phase C of the rotor in the case of a single-phase to ground fault in two modes: with PI controller and proposed controller

As can be seen from the results, when the PI controller is responsible for controlling the RSC, the amplitude of the rotor circuit current is increased to 1.6812 per units, while with the help of the proposed Fuzzy-PID controller, this current is limited to 1.532 per unit. Therefore, the simulation results guarantee the effectiveness of the proposed method.

4.2. Scenario 2

In this scenario, the DFIG is in its normal operating state, then a three-phase to ground fault occurs at 0.9 seconds in the middle of line A (15 Km from the beginning of the line 2) according to Fig. 8. This fault is resolved 0.1 seconds later with the function of the relay protection. The network voltage variations are very intense in this case as shown in Fig. 14.

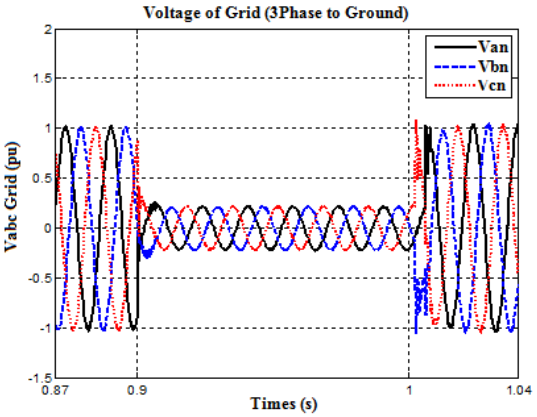

Figure 14: Network voltage in the case of a three-phase to ground fault

To compare the performance of the proposed controller based on the Fuzzy-PID controller with the PI controller in reducing the amplitude of the rotor circuit current, the current of each phase of the rotor circuit with each controller is plotted in Figs. 15 to 17.

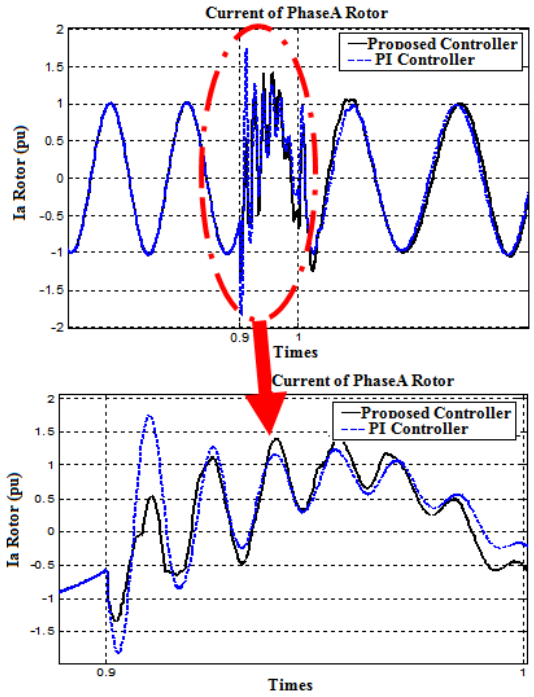

Figure 15: Comparison of the current of phase A of the rotor in the case of a three-phase to ground fault in two modes: with PI controller and proposed controller

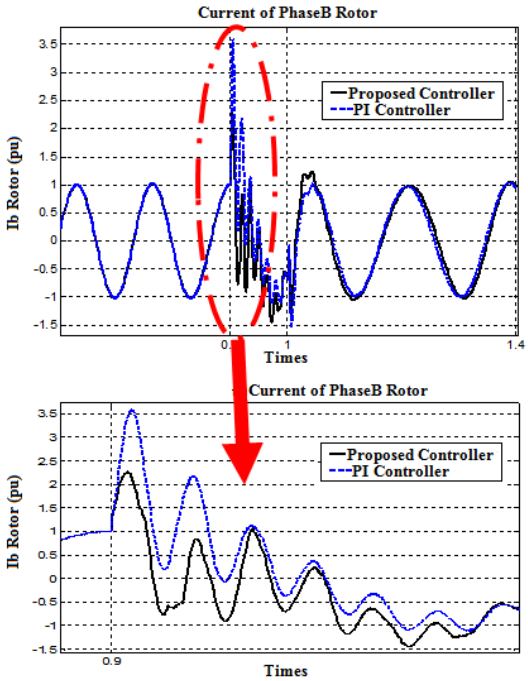

Figure 16: Comparison of the current of phase B of the rotor in the case of a three-phase to ground fault in two modes: with PI controller and proposed controller

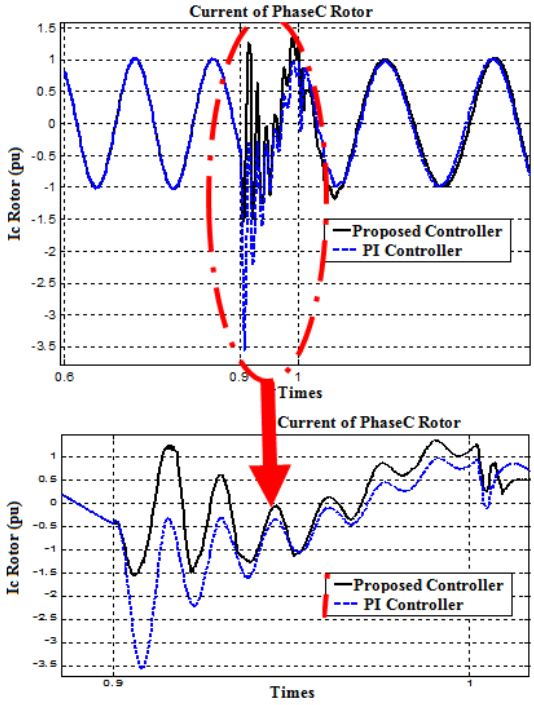

Figure 17: Comparison of the current of phase C of the rotor in the case of a three-phase to ground fault in two modes: with PI controller and proposed controller

As can be seen from the results, when the PI controller is responsible for controlling the RSC, the amplitude of the rotor circuit current is increased to 3.5980 per units, while with the help of the proposed Fuzzy-PID controller, this current is limited to 2.2840 per unit. Therefore, the simulation results guarantee the effectiveness of the proposed method.

5. Conclusions

In this article, a new control system based on Fuzzy-PID is presented to control the DFIG when a fault occurs in the network. The control system provided in this article has a very high performance speed and after adding to the system, quickly damps the transition conditions created by the fault and prevent high currents in the DFIG rotor and stator circuits. The suggested error observer has a desirable speed as well and can detect the fault only one thousandth of a second after the disturbance in the system.

References

[1] G. Abad, J. Lopez, M. Rodriguez, L. Marroyo and G. Iwanski, *Doubly fed Induction Machine: Modeling and Control for Wind Energy Generation*, Wiley-IEEE Press, 2011.

[2] R. Bhushan and K. Chatterjee, *Mathematical modeling and control of DFIG-based wind energy system by using optimized linear quadratic regulator weight matrices*, Int. Trans. Electr. Energ. Syst. 2017.

[3] M. Darabian and A. Jalilvand, *Predictive control strategy to improve stability of DFIG-based wind generation connected to a large-scale power system*, Int. Trans. Electr. Energ. Syst. 2017.

[4] S. Dhundhara and Y.P. Verma, *Evaluation of CES and DFIG unit in AGC of realistic multisource deregulated power system*, Int. Trans. Electr. Energ. Syst. 2017.

[5] I. Erlich, J. Kretschmann, J. Fortmann, S. Mueller-Engelhardt and H. Wrede, *Modeling of wind turbines based on doubly-fed induction generators for power system stability studies*, IEEE Trans. Power Sys. 22(3) (2007) 909–919.

[6] P.S. Flannery and G. Venkataramanan, *A fault tolerant doubly fed induction generator wind turbine using a parallel grid side rectifier and series grid side converter*, IEEE Trans. Power Elect. 23(3) (2008) 1126–1135.

[7] P.H. Huang, M.S. El Moursi, W. Xiao and J.L. Kirtley, *Subsynchronous resonance mitigation for series-compensated DFIG-based wind farm by using two-degree-of-freedom control strategy*, IEEE Trans. Power Syst. 30(3) (2015) 1442–1454.

[8] Y. Jin, J.E. Fletcher and J. O'Reilly, *A series-dynamic-resistor-based converter protection scheme for doubly-fed induction generator during various fault conditions*, IEEE Trans. Energy Conversion 25(2) (2010) 422–432.

[9] J.J. Justo, F. Mwasilu and J.W. Jung, *Doubly-fed induction generator based wind turbines: A comprehensive review of fault ride-through strategies*, Renewable and Sustainable Energy Rev., 45 (2015) 447–467.

[10] J. Lopez, E. Gubia, E. Olea, J. Ruiz and L. Marroyo, *Ride through of wind turbines with doubly fed induction generator under symmetrical voltage dips*, IEEE Trans. Indust. Elect. 56(10) (2009) 4246–4254.

[11] N.W. Miller, J.J. Sanchez-Gasca, W.W. Price and R.W. Delmerico, *Dynamic modeling of GE 1.5 and 3.6 MW wind turbine-generators for stability simulations*, IEEE Power Engin. Soc. General Meet. (2003) 1977–1983.

[12] R. Pena, J.C. Clare, G.M. Asher, *Doubly fed induction generator using back-to-back PWM converters and its application to variable-speed wind-energy generation*, IEE Proc. Electr. Power Appl. 143(3) (1996) 231–241.

[13] W. Qiao, G.K. Venayagamoorthy and R.G. Harley, *Real-time implementation of a sTATCOM on a wind farm equipped with doubly fed induction generators*, IEEE Trans. Indust. Appl. 45(1) (2009) 98–107.

[14] M.R. Shakarami, M. Joorabian and E. Afzalan, *Enhancement fault ride-through of DFIG with applications of ISM control for balance and unbalance voltage sag*, Comput. Intel. Elect. Engin. 9(3) (2018) 41–60.

[15] S.A. Taher, Z. Dehghani, M. Rahimi and M. Shahidehpour, *A new approach using combination of sliding mode control and feedback linearization for enhancing fault ride through capability of DFIG-based WT*, Int. Trans. Electr. Energ. Syst. (2018) 2613.

[16] M. Tsili and S. Papathanassiou, *A review of grid code technical requirements for wind farms*, IET Renewable Power Gener. 3(3) (2009) 308–332.